

SCIENTIFIC REPORTS



OPEN

Radiative transfer modelling reveals why canopy reflectance follows function

Teja Kattenborn  & Sebastian Schmidtlein

Optical remote sensing is potentially highly informative to track Earth's plant functional diversity. Yet, causal explanations of how and why plant functioning is expressed in canopy reflectance remain limited. Variation in canopy reflectance can be described by radiative transfer models (here PROSAIL) that incorporate plant traits affecting light transmission in canopies. To establish causal links between canopy reflectance and plant functioning, we investigate how two plant functional schemes, i.e. the Leaf Economic Spectrum (LES) and CSR plant strategies, are related to traits with relevance to reflectance. These traits indeed related to both functional schemes, whereas only traits describing leaf properties correlated with the LES. In contrast, traits related to canopy structure showed no correlation to the LES, but to CSR strategies, as the latter integrates both plant economics and size traits, rather than solely leaf economics. Multiple optically relevant traits featured comparable or higher correspondence to the CSR space than those traits originally used to allocate CSR scores. This evidences that plant functions and strategies are directly expressed in reflectance and entails that canopy 'reflectance follows function'. This opens up new possibilities to understand differences in plant functioning and to harness optical remote sensing data for monitoring Earth's functional diversity.

Through natural selection plants have diversified in various functions in order to adapt to environmental conditions, including abiotic factors (e.g. precipitation or nutrient gradients) and biotic interactions (e.g. competition or herbivory). Assessing patterns of plant functioning in space and time is a prerequisite to understand biosphere-atmosphere interactions and ecosystem dynamics such as community assembly or nutrient cycles¹⁻⁵. With accelerated global change the data demand on patterns of plant functioning has increased, as the latter is heavily affected by anthropogenic impacts⁶⁻⁹. However, due to vast temporal and spatial variation in plant functions, and the complexity to retrieve the latter in an explicit, consistent and spatially exhaustive way, data of Earth's plant functional diversity remain limited^{5,10}. To close this gap optical Earth observation data is potentially highly informative^{11,12}. During recent years, various studies have demonstrated that optical Earth observation data allows mapping variation in plant functioning, functional types and strategies¹³⁻²⁰. However, it often remains unclear why we can remotely sense differences in plant functioning^{11,21,22}. To fully harness the potential of Earth observation data and to improve available algorithms, it is crucial to understand the underlying processes that enable us to monitor plant functioning. The key to such understanding are the traits that contribute to canopy reflectance.

The mechanics of solar radiation in plant canopies, including light emitted from plant canopies and thus retrievable from Earth observation sensors, is already well understood and formulated in process-oriented models, i.e. canopy radiative transfer models (RTMs). Although radiative transfer is determined by traits with relevance for plant functioning, few studies have explicitly linked RTMs and plant functioning^{19,23,24}. Such RTMs are particularly determined by canopy characteristics defining the amount of light being intercepted or scattered by the foliage as well as foliage properties (e.g. leaf constituents or structure) defining leaf internal scattering, absorption and transmission rates. Here, we assess the distribution of these traits along plant functional gradients, because knowing more about the links between optically relevant traits and plant functioning allows for mapping and monitoring plant functions in a more mechanistic way. This could dramatically improve the robustness and transferability of our models. Furthermore, it can be assumed that bridging plant functioning and canopy reflectance with radiative transfer theory can increase our understanding of how environmental factors and biotic interactions shape plant functional diversity¹¹ (Fig. 1).

Institute of Geography and Geoecology (IFGG), Karlsruhe Institute of Technology (KIT), Kaiserstr. 12, 76131, Karlsruhe, Germany. Correspondence and requests for materials should be addressed to T.K. (email: teja.kattenborn@kit.edu)

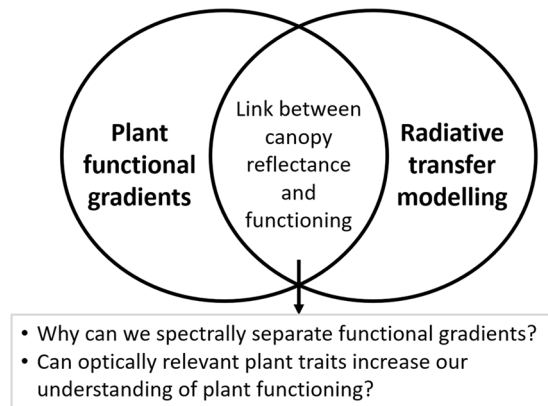


Figure 1. Rationale of linking plant functioning with radiative transfer modelling.

As optically relevant traits we addressed those traits that are incorporated in PROSAIL^{25–27}, which is the most widely applied RTM for plant canopies. It couples two models, firstly PROSPECT modelling the leaf optical properties (e.g. pigment or water content), and secondly 4SAIL taking into account the structural properties of a canopy (e.g. leaf orientation) and its relative orientation to the sun and sensor²⁵. We also considered traits that can be directly deduced from the original PROSAIL trait space (e.g. leaf pigments by leaf mass or fAPAR). A summary of traits and assumed links to plant functions is provided in Table 1.

We assessed the distribution of these traits across plant functional gradients using *in-situ* measurements acquired in an outdoor experimental setting with plants grown in pots. The species pool comprised 45 herbaceous species from Central Europe and covered a broad functional spectrum.

Instead of looking at individual functions such as carbon sequestration or evapotranspiration, we referred to more general expressions of plant functioning provided by two well-established schemes: the Leaf Economic Spectrum (LES³) and Grime's CSR model of plant strategy types (CSR^{28,29}). Both schemes are general approximations of principal functional differences between species that bundle many individual functions to metrics characterising their overall performance towards abiotic and biotic environmental selection pressures.

The LES was derived from analysing various leaf traits (leaf lifespan, leaf mass per area, photosynthetic capacity, dark respiration rate, nitrogen, and phosphorus concentration) and describes the spectrum of leaf resource investments ranging from fast and acquisitive (low investment) to slow and conservative growth (high investment) (Fig. 2a)³. We compared optically relevant traits to the LES, as resource economics in leaves have been found to reflect a main axis of functional differences in plants^{3,30} and can thus assumed to be directly linked to the optical leaf traits in PROSAIL. The CSR model characterises plant species by means of three axes, defining their competitive (C), stress tolerating (S) and ruderal abilities (R) (Fig. 2b)^{28,29}. Competitors are adapted to nutrient-rich sites featuring rapid growth to preempt resources. Stress-tolerators compensate environmental conditions limiting metabolic function through slow and robust growth, whereas ruderals are small-sized with short life cycles to counteract lethal events of disturbance or biomass removal. We compared optically relevant traits to the CSR scheme as it, in contrast to the LES, further integrates differences in function at the whole plant level^{29,31} and, thus, may be more appropriate for assessing optically relevant traits that are related to the canopy structure.

Results

Optically relevant traits versus Leaf Economic Spectrum. Which role do optically relevant traits play in relation to the LES? The set of optically relevant plant traits (compare Table 1) can be summarised using a three-dimensional feature space (Fig. 3), built by a principal component analysis, with component 1, 2 and 3 explaining 28%, 26% and 16% of the total variation, respectively. The LES was projected to this three-dimensional trait space to visualise relationships with optically relevant traits. As expected, LMA, as one of the original constituents of the LES, showed the highest correlation with the LES (-0.68 Pearson's r). A lower yet positive correlation ($p < 0.05$) existed with pigment contents measured on a mass basis, i.e. Cab_{mass} ($r = 0.42$), Car_{mass} ($r = 0.53$), Ant_{mass} ($r = 0.52$), indicating decreasing pigment concentrations with increasing resource investments. Pigments measured on an area-basis also correlated significantly but negatively with the LES, i.e. Cab_{area} ($r = -0.45$), Car_{area} ($r = -0.44$), so that pigment contents predominantly increased with slow and conservative growth. Mesophyll thickness N_{meso} correlated negatively with the LES ($r = -0.40$), reflecting higher mesophyll thickness with increasing resource investments. Traits linked to leaf water content (EWT , EWT_{canopy} , $LDMC$) and canopy structure (LAI , ALA , $fAPAR$, $APAR_{cum}$) were not significantly correlated to the LES. A table with all correlations is provided in S5.

Optically relevant traits versus CSR plant strategies. The distribution of optically relevant traits within the three-dimensional CSR scheme of plant strategies was assessed using thin plate regression splines³² and Generalized Additive Models (GAM)³³. Neither EWT nor EWT_{canopy} correlated to plant strategies among forbs or graminoids. In contrast LAI , LMA , LMA_{canopy} , $LDMC$, $pigment_{mass}$, $fAPAR$ and $APAR_{cum}$ showed significant and consistent relationships across forbs and graminoids (Fig. 4). $Pigment_{area}$, N_{meso} , C_{brown} and ALA exhibited no consistent relationship to CSR plant strategies across growth forms and thus related differently among forb and graminoid strategies (Figs 4–6). A table summarising the results for all traits is given in S6.

	Trait/Parameter [unit]	Abbr.	Description/functional role
Traits incorporated in PROSAIL-D	Chlorophyll content [$\mu\text{g}/\text{cm}^2$]	Cab_{area}	Leaf pigments chlorophyll a + b; primary molecule for light harvesting ²⁷
	Carotenoid content [$\mu\text{g}/\text{cm}^2$]	Car_{area}	Leaf pigments including xanthophylls and carotenes; photoprotection and light harvesting ²⁷
	Anthocyanin content [$\mu\text{g}/\text{cm}^2$]	Ant_{area}	Leaf pigments of the flavonoid family; photoprotection, protection from pathogens ^{58,72}
	Leaf Area Index [m^2/m^2]	LAI	Ratio of total one sided leaf area per unit ground; dominant control of primary productivity and transpiration ^{24,52,73}
	Leaf Inclination Distribution Function [deg.]	LIDF	Variation of leaf angles in the canopy; controls light harvesting efficiency, leaf temperature and transpiration ^{40,74}
	Leaf Mass per Area [g/cm^2]	LMA	Inverse of Specific Leaf Area (SLA), Aggregates leaf constituents such as sugar, starch, cellulose or lignin; well-known proxy for resource allocation and plant strategies ^{4,28}
	Equivalent Water Thickness [mg/cm^2]	EWT	Water content per leaf area; determines thermal regulation, drought resistance and flammability ⁷⁵⁻⁷⁷
	Mesophyll structure coefficient [-]	N_{meso}	Artificially designed PROSPECT parameter, relating to the thickness of the mesophyll layer, which affects light harvesting and light transmission as well as CO_2 diffusion ^{55,78}
Brown pigment content [-]	Cbrown	Artificial PROSPECT parameter, relates to polyphenols such as tannins and other secondary metabolites with functions such as UV protection or defensive compounds against herbivory and pathogens ^{79,80}	
Traits derived from PROSAIL-D trait space	Canopy Leaf Mass per Area [g/m^2]	$\text{LMA}_{\text{canopy}}$	Total leaf mass per canopy area [m^2] calculated as the product of LAI and LMA
	Canopy water content [g]	$\text{EWT}_{\text{canopy}}$	Total water content per canopy area [m^2] calculated as the product of LAI and EWT
	Chlorophyll conc. [%o]	Cab_{mass}	Chlorophyll mass per leaf dry mass
	Carotenoid conc. [%o]	Car_{mass}	Carotenoid mass per leaf dry mass
	Anthocyanin conc. [%o]	Ant_{mass}	Anthocyanin mass per leaf dry mass
	Fraction of Absorbed Photosynthetically Active Radiation [%]	fAPAR	Fraction of photosynthetic active radiation (PAR) absorbed in canopy. Integrates absorption by pigments and canopy structural traits (LAI, ALA); reflects gross photosynthetic capacity of the canopy. Simulated using PROSAIL (S3)
	Accumulated Absorbed PAR [kWh/m^2]	APAR_{cum}	PAR absorbed within the growing season; derived from multiplying fAPAR with course of direct and diffuse radiation during species specific growth length (S3)

Table 1. The optically relevant plant traits considered in the present study and their functions. These are traits implemented in PROSAIL and derivatives thereof.

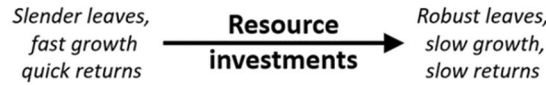
Discussion

Vegetation canopies can be considered as solar power plants and various functions and traits are coordinated to ensure an efficient energy assimilation by adapting to environmental factors (e.g. nutrient availability, temperature) and biotic interactions (e.g. competition)^{11,34}. Indeed, our results confirmed that plant functions and strategies are expressed through traits that directly affect or are directly related to optical processes in plant canopies and thus determine their reflectance. This relationship of ‘reflectance follows function’ firstly provides the physical basis for retrieving differences in plant functions by means of optical Earth observation data, and underlines the potential to track Earth’s functional diversity. Secondly, linking plant functions and strategies with radiative transfer provides a different and additional perspective on how environmental factors and biotic interactions shape plant functional diversity.

Why does reflectance of plant canopies follow function? Our results showed strong links between optically relevant plant traits and the two schemes used as baselines for plant functioning, i.e. the Leaf Economic Spectrum (LES) and CSR plant strategies. Originally the LES has been captured through leaf lifespan, LMA, photosynthetic capacity, dark respiration rate, nitrogen and phosphorus content³. Indeed, variation of observed LMA showed an strong correspondence to the LES, whereas we also found significant correlations with $\text{pigment}_{\text{mass}}$, and $\text{pigment}_{\text{area}}$, both of which are directly linked to photosynthetic capacity and nitrogen content³⁵. Our results further suggest that pigment content ($\text{pigment}_{\text{area}}$) generally increases with leaf lifespan, whereas the concentration of pigments ($\text{pigment}_{\text{mass}}$) decreases. Thus, plant investment in leaf tissue proportionally outweigh investment in leaf pigment, which can be explained as with increasing chlorophyll content light absorption follows a saturating curve, since chloroplasts become increasingly stacked in the palisade cells resulting in intraleaf shading³⁶⁻³⁸. Accordingly, plants with short leaf lifespan invest fewer pigment to optimise energy revenue. However, the LES reflects only one primary dimension of plant functioning, ranging from a quick to slow return on leaf resource investments. Accordingly, the canopy-structure-related traits (LAI, $\text{LMA}_{\text{canopy}}$, ALA, fAPAR or APAR_{cum}) showed no significant correspondence to the LES, suggesting that these traits are indeed related to other functional axes (Fig. 3). With the ‘global spectrum of plant form and function’ Diaz *et al.* have identified two major axes of plant functional convergence, with one axis reflecting leaf resource investments (LES) and the other axis reflecting plant and organ size-related traits. Accordingly, we expected that optically relevant traits integrating canopy properties are associated with the size-related axis. We actually observed such association between canopy-structure-related traits and the multidimensional CSR space, which characterises plant functioning in terms of competitive, stress tolerant and ruderal abilities at the whole plant level³¹. Accordingly, multiple traits that did not exhibit an association with the LES (e.g. LAI, $\text{LMA}_{\text{canopy}}$ or fAPAR), in turn showed a notable correspondence to the CSR space. Our results confirmed previous relationships between traits and the CSR space and exhibited gradients that have not been assessed before.

In agreement with pivotal formulations of the CSR scheme²⁹ and the allocation by Hodgson *et al.*³⁹, LMA was lowest for ruderal species and highest for stress tolerators, closely followed by competitors (Fig. 4). Leaf mass per canopy area, i.e. $\text{LMA}_{\text{canopy}}$ ($\text{LMA} \bullet \text{LAI}$), which was to our knowledge not compared to CSR strategies before,

a) Leaf Economic Spectrum (LES)



b) CSR plant strategies

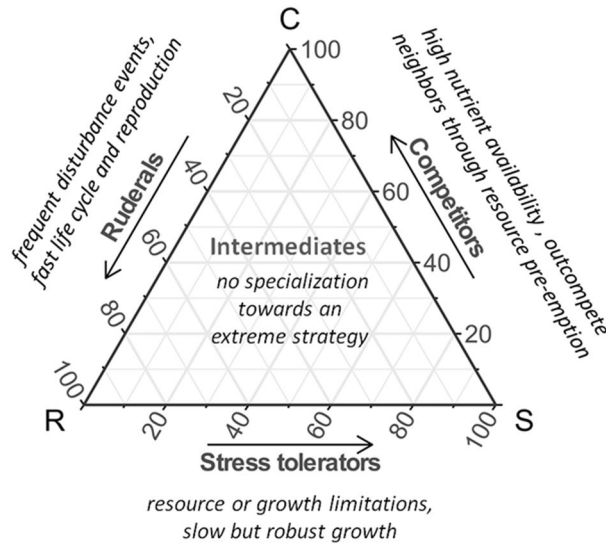


Figure 2. Schemes of plant functional gradients that were compared to optically relevant traits of cultivated plants: **(a)** Leaf Economic Spectrum (LES), and **(b)** CSR plant strategies.

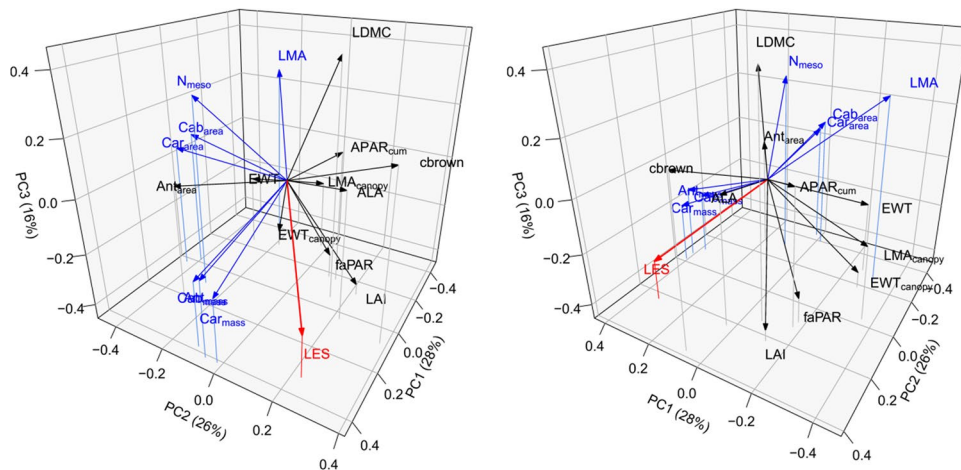


Figure 3. Two perspectives of the transformed trait space (principal component analysis) and relation to the Leaf Economic Spectrum (LES in red). Significant correlations between traits and the LES are highlighted in blue.

reflects total leaf carbon assimilation per canopy area. We found highest LMA_{canopy} for competitive species, followed by intermediate LMA_{canopy} for stress tolerators and intermediates and lowest values for ruderals. This gradient reflects the primary principles of the plant strategies²⁹; stress tolerators feature a conservative growth with a long leaf lifespan resulting in a steady accumulation of dry matter in the canopy, whereas ruderals are adapted to disturbance events and thus have short lifecycles in which they accumulate few resources. Competitors feature both high productivity and a relatively long lifespan and therefore highest resource accumulation (LMA_{canopy}).

Both leaf and canopy water content, i.e. EWT [g/cm^2] and EWT_{canopy} , did not show a clear relationship with plant strategies. In contrast $LDMC$, which is the ratio of leaf mass and leaf water content ($LDMC = LMA / (LMA + EWT)$), showed a clear coherence towards plant strategies and was therefore already used by Hodgson *et al.*³⁹

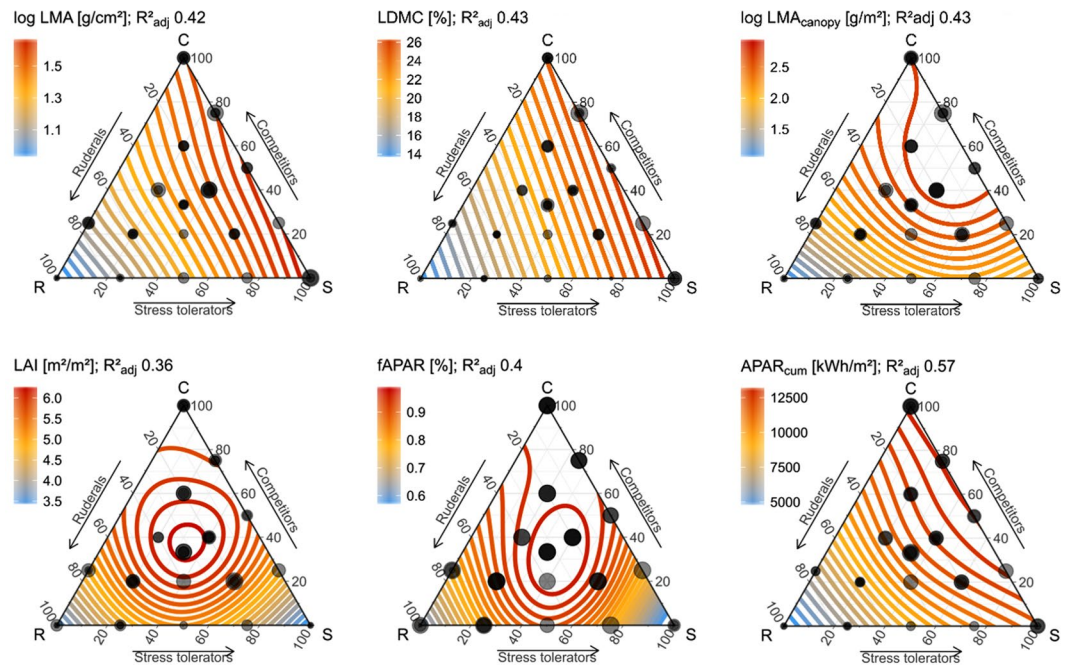


Figure 4. Distribution of optically relevant plant traits in the CSR- feature space of forbs and graminoids based on GAM extrapolations. Observations are displayed as transparent grey dots (partly overlapping) with a size proportional to the trait expression.

to allocate CSR scores. This suggests that functional characteristics are expressed through the relative water concentration in leaf tissue, rather than the absolute leaf water content.

A more complex pattern was found for LAI, where intermediate species (CSR) have highest LAI values followed by competitors, and lowest LAI values correspond to high S and R scores. We thus expect that intermediate species (CSR) invest a large share of resources in foliage area, whereas competitors, ruderals and stress tolerators invest more resources towards their strategy-specific trait-expressions and functions. Competitors occur primarily in nutrient rich sites, where competition for sunlight is most pronounced and triggers increased height growth to overtop neighbouring individuals. Increased canopy height in turn requires additional resource investments in support tissues, e.g. in the stem for vertical plant growth itself as well as in enhanced leaf robustness (higher LMA), to compensate for increased exposure to wind (compare LMA gradient, Fig. 4)⁴⁰. An increased LMA was also found for plants adapted to high light intensities (competitors) through increased palisade parenchyma to maximise photosynthetic capacity and thus quantum yield per unit leaf area and reduce potential light saturation^{41,42}. This suggests that relative to intermediate strategies, competitors invest fewer resources in the development of total foliage area (LAI). Therefore, competition for sunlight might enforce a trade-off between the maximisation of height growth and light interception. This agrees with Porter *et al.*⁴³, who have reported higher accumulation of leaves for shade tolerant species leaves with smaller canopy heights among tropical tree species.

Leaf inclination (ALA) did not show a trivial correspondence to the CSR spectrum, but differed between growth forms, reflecting generic differences in the canopy architecture of graminoids and forbs. Variation in leaf angles across graminoid strategies showed no explicit pattern. For forb strategies ALA increased from competitive forbs to stress tolerant and ruderal forbs (Fig. 5). This agrees with Hikosaka & Hirose⁴⁴, who have simulated leaf angle distributions for plant canopies and found lower leaf angles with increasing competition. Competitive forbs, which aim to overtop and shade out the surrounding and competing plants, develop rather flat leaf angles to deplete or scatter most of the light before it is available for rivals. However, a horizontal leaf position requires increased support costs for petioles and branches, and is generally less efficient for light absorption as self-shading and light saturation increases^{44,45}. Leaf angles hence increase with decreasing competition to scatter light between leaves and hence distribute light into the lower canopy^{44,46}.

Similar to the LES-based analysis, the derived distributions of chlorophylls, carotenoids and anthocyanins across the CSR space are very alike (Figs 4, S6), since pigments are usually highly correlated in mature leaves²⁷. Yet, the relationships differed greatly among pigments measured on an area basis (**pigment_{area}**) and measured on a mass basis (**pigment_{mass}**, Figs 6, S6). The relationship between pigment_{area} and CSR strategies further differed between forbs and graminoids (Fig. 6), which agrees with Tjoelker *et al.*⁴⁷, who has found differences in leaf photosynthetic activity between grasses and forbs. For forbs ruderals and intermediates feature highest pigment_{area}. Among graminoid strategies pigment_{area} showed a low and inconclusive variation across the CSR space apart from a strong increase for extremely stress tolerant graminoids (*Festuca ovina* and *Nardus stricta*).

Pigments normalised by mass (pigment_{mass}) showed a very consistent gradient across growth forms (S8), which however almost exclusively mirrors the LMA gradient (r^2 of 0.74, 0.80, 0.85 for Cab_{mass}, Car_{mass}, Ant_{mass}, respectively). This is further confirmed as the modelled pigment_{mass} values across the CSR-space were highly

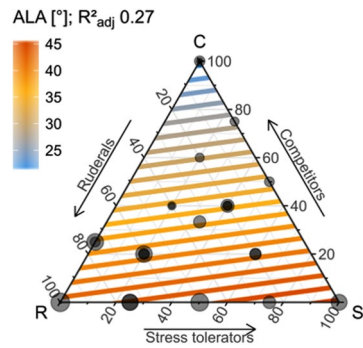


Figure 5. Distribution of average leaf angle (ALA) in the herbaceous CSR- feature space based on GAM extrapolations (details see caption Fig. 4).

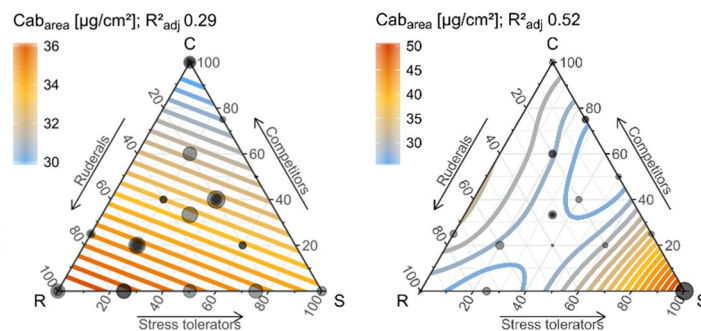


Figure 6. Distribution of Cab_{area} for herbaceous (left) and graminoid (right) CSR plant strategies based on GAM extrapolations (details see caption Fig. 4).

correlated with $pigments_{mass}$ values based on a null-model, in which we sampled random $pigments_{area}$ values that were subsequently divided by LMA and thus mass normalised (r^2 of 0.80, 0.91, 0.64 for Cab_{mass} , Car_{mass} , Ant_{mass} , respectively). Accordingly, we found that $pigments_{mass}$ indeed do not reflect pigment variation per se, but rather the LMA gradient, which varies in higher magnitudes than traits with photosynthetic function^{48,49}. Likewise the strong correspondence between $pigments_{mass}$ and the LES can largely be attributed by the high variation in LMA, as indicated by the null-model (S9). This indicates that the characterisation of plant canopies through pigments on a mass basis is greatly redundant with LMA and therefore appears to be not expedient, despite its frequent use in the remote sensing community^{50,51}.

The distribution of simulated $fAPAR$ across the CSR space showed a strong correspondence to LAI (Fig. 4), suggesting that variation in light harvesting is particularly determined by LAI (in line with^{44,46,52}) and therefore highest for intermediate strategies followed by competitors. Yet, $fAPAR$ solely represents the potential energy gain at a point in time and thereby does not consider phenological differences between plant strategies. Accordingly we modelled the accumulated photosynthetic active radiation $APAR_{cum}$. This measure integrates $fAPAR$ and the course of absorbed direct and diffuse radiation (assessed from HelioClim-3 archives⁵³) during a plants phenological season (recorded for the cultivated plants). $APAR_{cum}$ thus reflects the accumulated photosynthetic and carbon assimilation during a plant's growth period⁵⁴. $APAR_{cum}$ showed a very consistent and clear pattern across growth forms. Corresponding to their short growth period ruderalists featured the lowest $APAR_{cum}$. Intermediate $APAR_{cum}$ was found for stress tolerators, as these can compensate conditions that limit productivity through robustness and persistence, resulting in a comparably low but prolonged light harvesting. Highest $APAR_{cum}$ was found for competitors, as competitive abilities require long-term investments (e.g., height growth) that are rewarded with long-term returns. These results thus showed that the phenology-dependent variation in energy acquisition directly reflects established plant strategies and functions. Moreover, the comparable strong relationship with $APAR_{cum}$ emphasised that gradients in plant productivity are not fully reflected by a single biochemical or structural trait, but relate to the integrated response of pigments, LAI, ALA as well as phenology²². This particularly highlights the potential of multi-temporal Earth observation data to map functional gradients. The overall strong correlation between gradients derived from $APAR_{cum}$ and LMA_{canopy} ($r^2 = 0.88$) underlines the plausibility of the models, as a large share of the absorbed energy is used for carbon assimilation in leaves³⁵. The minor discrepancy between $APAR_{cum}$ and LMA_{canopy} existed for competitors, where photosynthetic assimilation ($APAR_{cum}$) is highest, but LMA_{canopy} showed a slight bias towards C-CSR, which could result from competitors investing a considerable part of their resources in height growth rather than total leaf tissue.

According to our results **Cbrown** and N_{meso} did not show a consistent relation with the CSR strategies across growth forms. Both traits only corresponded to CSR strategies among graminoids (S7). In agreement with Jacquemoud & Baret⁵⁵ N_{meso} correlates with LMA. The distribution of **Cbrown** could not be explained in an

ecological context. Overall, C_{brown} and N_{meso} have a relatively low impact on canopy reflectance⁵⁶ and do not greatly contribute to the spectral differentiation of variations in plant functioning⁵⁷.

All trait measurements used in this study were retrieved from plants cultivated under optimal growth conditions. It can be expected that some traits more explicitly express their functional role under non-optimal environmental conditions. For instance, increased leaf anthocyanin content has been observed during pathogen infections⁵⁸. Furthermore, a plant's ability to cope with excess incident radiation can be expressed through developing ample leaf carotenoid content²⁷.

A limitation of our study was the initial definition and selection of plant traits. Plant traits such as Leaf Area Index and the Average Leaf Angle are abstractions of complex canopy structural properties, and may not fully reflect subtle differences in plant functioning. Further errors are introduced by the trait measurements and the analysis, such as GAM extrapolations, and the abstraction of plant functioning in the CSR model²⁹ and the LES³. Yet, given that plant functioning and the radiative transfer in plant canopies are two complex fields on its own, empirically testing the links between these two realms requires a certain level of abstraction. Despite these uncertainties, our results showed unprecedented links between functioning and reflectance, hopefully triggering further advances towards this field using more sophisticated methods.

Conclusion and Outlook

Optical remote sensing data is potentially highly informative to track Earth's functional diversity. Yet, causal explanations on why plant functioning can be differentiated using canopy reflectance sensed by optical Earth observation data remain limited. Our findings demonstrate that bridging ecological theory and canopy reflectance through radiative transfer modelling enables us to identify causal links between canopy reflectance and plant functioning. These links suggest that canopy 'reflectance follows function', meaning that adaptations of plants to their environment are directly 'reflected' in their optical properties across the visible, near and short wave infrared wavelengths. More specifically plant functions and strategies are considerably expressed through multiple structural, physiological and phenological traits with relevance for canopy reflectance and thus optical Earth observation data. This opens up new opportunities for understanding plant functional changes in space and time. Increasing the dimension of relevant traits for an ecological system allows us to more precisely and completely understand and predict ecosystem dynamics and ecological processes such as community assembly⁵⁹. Furthermore, trait ecology may lack a sufficient variety of traits to capture dissimilarities and explain competition among species⁶⁰. As shown here optically relevant traits depict variations in multiple plant functions and can thus complement the suite of determinable proxies to describe spatial variation in plant functioning and community assembly. This is particularly emphasised as several optically relevant traits show comparable or even stronger correlations with CSR plant strategies (LAI , LMA_{canopy} , $APAR_{\text{cum}}$) than traits used originally to allocate the CSR space (e.g. LMA or $LDMC$ ³⁹). Upcoming hyperspectral satellite missions such as EnMAP⁶¹ or HypSI⁶² will provide optical reflectance products that are sensitive to the traits considered in this study. Our results therefore encourage further research to deepen our understanding how plant functioning is expressed through optically relevant traits using more extensive trait data and further traits incorporated in more complex radiative transfer models (e.g., crown architecture), such as INFORM⁶³ or FLIGHT⁶⁴.

Material and Methods

Retrieval of the traits space implemented in PROSAIL. We derived the PROSAIL trait space from outdoor cultivated plants, including 45 forb and graminoid species covering the full range of the CSR spectrum (Table 2). We performed seed propagation in greenhouses and moved the plants outdoor for a week of acclimatisation once they were grown to an adequate size. Afterwards the plants were planted out in four repetitions in separate pots with a size of 0.4 m • 0.4 m and 30 l volume filled with a standardised substrate. Fewer repetitions had to be planted for species where seedling propagation was less successful. All pots were regularly fertilised, weeded and irrigated.

For each species we measured the considered traits on a weekly basis for each pot. We determined the species-specific trait expressions by averaging the measurements among pots and subsequently calculating the median for the whole season. We only considered measurements that were performed in non-senescent canopies of adult plants (here defined as plants with closed canopy).

In view of the envisaged amount of measurements per species traditional approaches for pigment retrieval such as the spectrophotometer method by Lichtenthaler⁶⁵ was not feasible. Furthermore, N_{meso} and C_{brown} are specific parameters of PROSPECT. We measured leaf chlorophyll content (Cab_{area}), carotenoid content (Car_{area}), anthocyanin content (Ant_{area}), mesophyll structure coefficient (N_{meso}) and brown pigment content (C_{brown}) using leaf reflectance spectra and their inversion using the leaf radiative transfer model PROSPECT-D²⁷. We acquired leaf spectra of 5 individual leaves per cultivated pot using an ASD FieldSpec III (ASD, Inc. Boulder, CO, USA) attached with a plant probe and leaf clip. If the area of a leaf was smaller than the opening of the plant probe (3.14 cm²) we seamlessly, and without overlap, placed the leaves side by side on an adhesive tape. The inversion of PROSPECT-D was based on a look-up-table approach and wavelets^{66–68}. Further details on the inversion procedure and its validation are given in S1.

We estimated LAI using an Accu-PAR LP-80 ceptometer equipped with an external reference sensor to account for the current photosynthetic active radiation (PAR). For each pot we recorded and subsequently averaged 18 individual measurements.

To limited the destructive impact over time, we measured leaf mass per area (LMA) and equivalent water thickness (EWT) per species rather than per pot. Samples consist of leaflets only without petioles and rachis. Fresh leaf mass of around 10 g of whole leaves per species was measured on site. Total leaf area of these leaf samples was retrieved using a flatbed scanner. The LMA [g/cm²] was derived by drying the sample material at 70 °C for at least 72 h. EWT [mg/cm²] was derived by subtracting LMA from leaf fresh mass per area.

Graminoids (n = 20)	Forbs (n = 25)
<i>Alopecurus geniculatus</i> (4, R/CSR); <i>Alopecurus pratensis</i> (4, C/CSR); <i>Anthoxanthum odoratum</i> (4, SR/CSR); <i>Apera spica-venti</i> (4, R/SR); <i>Agrostis capillaris</i> (4, CSR); <i>Arrhenatherum elatius</i> (4, C/CSR); <i>Brachypodium sylvaticum</i> (4, S/SC); <i>Bromus hordeaceus</i> (3, R/CR); <i>Calamagrostis epigejos</i> (4, C/SC); <i>Deschampsia cespitosa</i> (4, S/CSR); <i>Digitaria sanguinalis</i> (4, R/SR); <i>Festuca ovina</i> (4, S); <i>Holcus lanatus</i> (4, CSR); <i>Luzula multiflora</i> (4, S/CSR); <i>Molinia caerulea</i> (2, SC); <i>Nardus stricta</i> (4, S); <i>Phalaris arundinacea</i> (4, C); <i>Poa annua</i> (4, R); <i>Scirpus sylvaticus</i> (4, C/SC); <i>Trisetum flavescens</i> (4, CSR);	<i>Aegopodium podagraria</i> (4, CR/CSR); <i>Anthyllis vulneraria</i> (2, S/SR); <i>Arctium lappa</i> (4, C); <i>Centaurium erythraea</i> (4, SR); <i>Cirsium arvense</i> (4, C); <i>Cirsium acaule</i> (3, CS/CSR); <i>Digitalis purpurea</i> (4, CR/CSR); <i>Filipendula ulmaria</i> (1, C/SC); <i>Geum urbanum</i> (4, S/CSR); <i>Geranium pratense</i> (4, C/CSR); <i>Geranium robertianum</i> (R/CSR); <i>Plantago major</i> (4, R/CSR); <i>Clinopodium vulgare</i> (4, S/CSR); <i>Campanula rotundifolia</i> (4, S); <i>Lamium purpureum</i> (4, R); <i>Lapsana communis</i> (4, R/CR); <i>Medicago lupulina</i> (3, R/SR); <i>Origanum vulgare</i> (4, CS/CSR); <i>Pulicaria dysenterica</i> (4, CS); <i>Stellaria media</i> (4, R/CR); <i>Succisa pratensis</i> (3, CS/CSR); <i>Taraxacum spec.</i> (4, R/CSR); <i>Thlaspi arvense</i> (3, R); <i>Trifolium pratense</i> (4, CSR); <i>Urtica dioica</i> (4, C);

Table 2. List of all cultivated species. The number in parentheses indicates the number of repetitions per species followed by the allocated CSR strategy.

The ALA was retrieved from leaf inclination distributions that we determined using levelled digital photograph and the procedure described by Ryu *et al.*⁶⁹. For each species we measured not less than 50 angles of leaves parallel to the viewing direction. Leaf angle distributions and ALA were only retrieved once due to logistic constrains.

We deduced additional traits from the PROSAIL traits space to further exploit its information content: leaf dry matter content ($LDMC = LMA / (LMA + EWT)$); canopy leaf mass per area ($LMA_{\text{canopy}} = LMA \bullet LAI$); canopy pigment content ($\text{pigment}_{\text{canopy}} = \text{pigment}_{\text{area}} \bullet LAI$); fraction of absorbed photosynthetic active radiation ($fAPAR$) simulated using PROSAIL (details in S3)²⁵; cumulative absorbed photosynthetic active radiation ($APAR_{\text{cum}}$ in kWh/m^2), which corresponds to the total absorbed energy within the growing season of each species. The $APAR_{\text{cum}}$ was calculated as the product of $fAPAR$, direct and diffuse irradiance averaged for April-October (data assessed from HelioClim-3 data⁵³, details in S3) and the length of the growing season, (here defined as the observed number of weeks between maturity and senescence). A statistical summary of the trait space is given in S2.

Linking the Leaf Economic Spectrum and optically relevant plant traits. Wright *et al.*³ determined the LES using the first component of a principal component transformation of six leaf traits, i.e. LMA, photosynthetic assimilation rate_{mass}, leaf nitrogen_{mass}, leaf phosphorus_{mass}, dark respiration rate_{mass}, and leaf lifespan. From those traits we only measured LMA (or SLA respectively) within the above described plant experiment. We therefore requested the remaining traits from the TRY-database, where sufficient data was available for 26 of the 45 species (see S4 for a list of the 26 species) and two further traits, leaf nitrogen_{mass}, leaf phosphorus_{mass}. We determined the LES for the 26 species using the log10 transformed expressions of these three traits and the loadings reported by Wright *et al.*³. The LES retrieved this way was compared to each of the optically relevant traits using Pearson's correlation coefficient. Additionally, the relationship among the different optically relevant traits and their relation to the LES was visualised by means of a principal component analysis (PCA). Therefore, we built a PCA of the PROSAIL trait space on which the LES was projected using the function ('envfit' of the vegan package). Prior to the PCA the PROSAIL traits were centered and scaled.

Linking CSR plant strategies and optically relevant plant traits. The position of a species in the CSR space is defined by three axes expressing competitive, stress tolerant and ruderal abilities (scores). We used the CSR scores provided by Hodgson *et al.*³⁹, who allocated CSR strategies for a multitude of European plant species using trait expressions of canopy height, LDMC, flowering period, flowering start, lateral spread, LMA and specific leaf area (Table 2). For some species we adopted the allocation from the BioFlor database⁷⁰ and expert knowledge.

We assessed the relationship between each PROSAIL trait and the CSR space using Generalized Additive Models (GAM)³³ and thin plate regression splines³². As input for the GAM we used the first two PCA components (cumulative variance 97%) instead of the raw CSR scores to facilitate the interpretability of the results. The results were visualised in ternary plots (R-package 'ggtern')⁷¹.

References

- Díaz, S. & Cabido, M. Vive la difference: plant functional diversity matters to ecosystem processes. *Trends in Ecology & Evolution* **16**(11), 646–655 (2001).
- Bonan, G. B., Levis, S., Kergoat, L. & Oleson, K. W. Landscapes as patches of plant functional types: An integrating concept for climate and ecosystem models. *Global Biogeochemical Cycles*, **16**(2) (2002).
- Wright, I. J., Reich, P. B., Westoby, M. & Ackerly, D. D. The worldwide leaf economics spectrum. *Nature* **428**(6985), 821 (2004).
- Reichstein, M., Bahn, M., Mahecha, M. D., Kattge, J. & Baldocchi, D. D. Linking plant and ecosystem functional biogeography. *Proceedings of the National Academy of Sciences of the USA* **111**(38), 13697–13702 (2014).
- Violle, C., Reich, P. B., Pacala, S. W., Enquist, B. J. & Kattge, J. The emergence and promise of functional biogeography. *Proceedings of the National Academy of Sciences of the USA* **111**(38), 13690–13696 (2014).
- Chapin, F. S. *et al.* Biotic control over the functioning of ecosystems. *Science* **277**(5325), 500–504 (1997).
- Cramer, W. *et al.* Global response of terrestrial ecosystem structure and function to CO² and climate change: results from six dynamic global vegetation models. *Global Change Biology* **7**(4), 357–373 (2001).
- Braat, L. C., ten Brink, P. E. & Klok, T. C. The Cost of Policy Inaction: The case of not meeting the 2010 biodiversity target. *Alterra*, 1718 (2008).
- Cardinale, B. J. *et al.* Biodiversity loss and its impact on humanity. *Nature* **486**(7401), 59 (2012).
- Kattge, J. *et al.* TRY—a global database of plant traits. *Global Change Biology* **17**(9), 2905–2935 (2011).
- Ustin, S. L. & Gamon, J. A. Remote sensing of plant functional types. *New Phytologist* **186**(4), 795–816 (2010).
- Homolová, L., Malenovský, Z., Clevers, J. G. P. W., Garcia-Santos, G. & Schaepman, M. E. Review of optical-based remote sensing for plant trait mapping. *Ecological Complexity* **15**, 1–16 (2013).

13. Schmidtlein, S. Imaging spectroscopy as a tool for mapping Ellenberg indicator values. *Journal of Applied Ecology* **42**(5), 966–974 (2005).
14. Baret, F. *et al.* LAI, fAPAR and fCover CYCLOPES global products derived from VEGETATION: Part 1: Principles of the algorithm. *Remote Sensing of Environment* **110**(3), 275–286 (2007).
15. Hilker, T., Coops, N. C., Wulder, M. A., Black, T. A. & Guy, R. D. The use of remote sensing in light use efficiency based models of gross primary production: A review of current status and future requirements. *Science of the Total Environment* **404**(2–3), 411–423 (2008).
16. Friedl, M. A. *et al.* MODIS Collection 5 global land cover: Algorithm refinements and characterization of new datasets. *Remote sensing of Environment* **114**(1), 168–182 (2010).
17. White, M. A. *et al.* Intercomparison, interpretation, and assessment of spring phenology in North America estimated from remote sensing for 1982–2006. *Global Change Biology* **15**(10), 2335–2359 (2009).
18. Schmidtlein, S., Feilhauer, H. & Bruehlheide, H. Mapping plant strategy types using remote sensing. *Journal of Vegetation Science* **23**(3), 395–405 (2012).
19. Feilhauer, H., Doktor, D., Schmidtlein, S. & Skidmore, A. K. Mapping pollination types with remote sensing. *Journal of Vegetation Science* **27**(5), 999–1011 (2016).
20. Garbulsky, M. F., Peñuelas, J., Gamon, J., Inoue, Y. & Filella, I. The photochemical reflectance index (PRI) and the remote sensing of leaf, canopy and ecosystem radiation use efficiencies: A review and meta-analysis. *Remote Sensing of Environment* **115**(2), 281–297 (2011).
21. Schaepman, M. E. *et al.* Earth system science related imaging spectroscopy—An assessment. *Remote Sensing of Environment* **113**(1), 123–137 (2009).
22. Ollinger, S. V. Sources of variability in canopy reflectance and the convergent properties of plants. *New Phytologist* **189**(2), 375–394 (2011).
23. Ali, A. M. *et al.* Retrieval of forest leaf functional traits from HySpex imagery using radiative transfer models and continuous wavelet analysis. *ISPRS Journal of Photogrammetry and Remote Sensing* **122**, 68–80 (2016).
24. Kattenborn, T. *et al.* Linking plant strategies and plant traits derived by radiative transfer modelling. *Journal of Vegetation Science*, **28**(4) (2017).
25. Verhoef, W. & Bach, H. Coupled soil–leaf–canopy and atmosphere radiative transfer modeling to simulate hyperspectral multi-angular surface reflectance and TOA radiance data. *Remote Sensing of Environment* **109**(2), 166–182 (2007).
26. Jacquemoud, S. *et al.* PROSPECT+ SAIL models: A review of use for vegetation characterization. *Remote sensing of Environment* **113**, 56–66 (2009).
27. Féret, J.-B., Gitelson, A. A., Noble, S. D. & Jacquemoud, S. PROSPECT-D: Towards modeling leaf optical properties through a complete lifecycle. *Remote Sensing of Environment* **193**, 204–215 (2017).
28. Pierce, S. *et al.* A global method for calculating plant CSR ecological strategies applied across biomes world wide. *Functional Ecology* **31**(2), 444–457 (2017).
29. Grime, J. P. *et al.* Integrated screening validates primary axes of specialization in plants. *Oikos* **79**, 259–281 (1997).
30. Díaz, S. *et al.* The global spectrum of plant form and function. *Nature* **529**(7585), 1–17 (2016).
31. Pierce, S. & Cerabolini, B. E. Plant economics and size trait spectra are both explained by one theory (open-access self-published essay). *Plant Press* (2018).
32. Wood, S. N. Thin plate regression splines. *J.R.Statist.Soc.B* **65**(1), 95–114 (2003).
33. Hastie, T. & Tibshirani, R. Generalized Additive Models. *Statistical Science* **1**(3), 297–318 (1986).
34. Ehleringer, J. S. & Werk, K. S. Modifications of solar-radiation absorption patterns and implications for carbon gain at the leaf level. In: Givnish T. J., ed. *On the economy of plant form and function*. Cambridge, UK: Cambridge University Press, 57–82 (1986).
35. Lambers, H., Chapin, F. S. & Pons, T. L. *Plant Physiological Ecology*, Springer, New York (1998).
36. Terashima, I. & Hirose, K. Comparative ecophysiology of leaf and canopy photosynthesis. *Plant, Cell and Environment* **18**, 1111–1128 (1995).
37. Evans J. R. Developmental constraints on photosynthesis: Effects of light and nutrition. In *Photosynthesis and the Environment* (ed. Baker, N. R.), pp. 281–304. Kluwer, Dordrecht, Netherlands (1996).
38. Evans, J. R. & Poorter, H. Photosynthetic acclimation of plants to growth irradiance: The relative importance of specific leaf area and nitrogen partitioning in maximizing carbon gain. *Plant, Cell and Environment* **24**(8), 755–767 (2001).
39. Hodgson, J. G. *et al.* Plant functional types: a soft approach to a hard problem. *Oikos*, 282–294 (1999).
40. Niinemets, Ü. A review of light interception in plant stands from leaf to canopy in different plant functional types and in species with varying shade tolerance. *Ecological Research* **25**(4), 693–714 (2010).
41. Björkman, O. Responses to different quantum flux densities. In *Physiological Plant Ecology I* (pp. 57–107). Springer, Berlin, Heidelberg (1981).
42. Poorter, H., Niinemets, Ü., Poorter, L., Wright, I. J. & Villar, R. Causes and consequences of variation in leaf mass per area (LMA): a meta analysis. *New Phytologist* **182**(3), 565–588 (2009).
43. Poorter, L., Bongers, L. & Bongers, F. Architecture of 54 moist forest tree species: traits, trade-offs, and functional groups. *Ecology* **87**(5), 1289–1301 (2006).
44. Hirose, K. & Hirose, T. Leaf angle as a strategy for light competition: Optimal and evolutionarily stable light-extinction coefficient within a leaf canopy. *Ecoscience* **4**(4), 501–507 (1997).
45. Niklas, K. J. *Plant allometry: the scaling of form and process*. University of Chicago Press (1994).
46. Hümmrich, K. F. Simulations of Seasonal and Latitudinal Variations in Leaf Inclination Angle Distribution: Implications for Remote Sensing. *Advances in Remote Sensing* **2**(2), 93–101 (2013).
47. Tjoelker, M. G., Craine, J. M., Wedin, D., Reich, P. B. & Tilman, D. Linking leaf and root trait syndromes among 39 grassland and savannah species. *New Phytologist* **167**(2), 493–508 (2005).
48. Osnas, J. L., Lichstein, J. W., Reich, P. B. & Pacala, S. W. Global leaf trait relationships: mass, area, and the leaf economics spectrum. *Science* **340**(6133), 741–744 (2013).
49. Lloyd, J., Bloomfield, K., Domingues, T. F. & Farquhar, G. D. Photosynthetically relevant foliar traits correlating better on a mass vs an area basis: Of ecophysiological relevance or just a case of mathematical imperatives and statistical quicksand? *New Phytologist* **199**(2), 311–321 (2013).
50. Asner, G. P. & Martin, R. E. Airborne spectranomics: mapping canopy chemical and taxonomic diversity in tropical forests. *Frontiers in Ecology and the Environment* **7**(5), 269–276 (2009).
51. Jetz, W. *et al.* Monitoring plant functional diversity from space. *Nature Plants* **2**(3), 16024 (2016).
52. Asner, G. P., Scurlock, J. M. & Hicke, J. A. Global synthesis of leaf area index observations: implications for ecological and remote sensing studies. *Global Ecology and Biogeography* **12**, 191–205 (2003).
53. Espinar, B. *et al.* HelioClim-3: a near-real time and long-term surface solar irradiance database. Workshop on *Remote Sensing Measurements for Renewable Energy* (2012).
54. Goward, S. N., Tucker, C. J. & Dye, D. G. North American vegetation patterns observed with the NOAA-7 advanced very high resolution radiometer. *Vegetatio* **64**, 3–14 (1985).
55. Jacquemoud, S. & Baret, F. PROSPECT: A model of leaf optical properties spectra. *Remote Sensing of Environment* **34**(2), 75–91 (1990).
56. Jacquemoud, S. Inversion of the PROSPECT+ SAIL canopy reflectance model from AVIRIS equivalent spectra: theoretical study. *Remote sensing of environment* **44**(2–3), 281–292 (1993).

57. Kattenborn, T., Fassnacht, F. E. & Schmidlein, S. Differentiating plant functional types using reflectance: Which traits make the difference? *Remote Sensing in Ecology and Conservation* **5**(1), 5–19 (2018).
58. Zarco-Tejada, P. J. *et al.* Previsual symptoms of Xylella fastidiosa infection revealed in spectral plant-trait alterations. *Nature Plants* **4**(7), 432 (2018).
59. Reich, P. B. The world wide ‘fast–slow’ plant economics spectrum: a traits manifesto. *Journal of Ecology*, **102**(2), 275–301 (2014).
60. Kunstler, G. *et al.* Plant functional traits have globally consistent effects on competition. *Nature* **529**(7585), 204–207 (2016).
61. Stuffer, T. *et al.* The EnMAP hyperspectral imager—An advanced optical payload for future applications in Earth observation programmes. *Acta Astronautica* **61**(1), 115–120 (2007).
62. Roberts, D. A., Quattrochi, D. A., Hulley, G. C., Hook, S. J. & Green, R. O. Synergies between VSWIR and TIR data for the urban environment: An evaluation of the potential for the Hyperspectral Infrared Imager (HypSIIRI) Decadal Survey mission. *Remote Sensing of Environment* **117**, 83–101 (2012).
63. Atzberger, C. Development of an invertible forest reflectance model: The INFOR-Model. In: Buchroithner (Ed.): *A decade of trans-european remote sensing cooperation*. Proceedings of the 20th EARSeL Symposium Dresden, Germany, 39–44 (2000).
64. North, P. R. J. Three-dimensional forest light interaction model using a Monte Carlo method. *IEEE Transactions on Geoscience and Remote Sensing* **34**, 946–956 (1996).
65. Lichtenthaler, H. K. Chlorophylls and carotenoids: pigments of photosynthetic biomembranes. *Methods in Enzymology* **148**, 350–382 (1987).
66. Blackburn, G. A. Wavelet decomposition of hyperspectral data: a novel approach to quantifying pigment concentrations in vegetation. *International Journal of Remote Sensing* **28**(12), 2831–2855 (2007).
67. Blackburn, G. A. & Ferwerda, J. G. Retrieval of chlorophyll concentration from leaf reflectance spectra using wavelet analysis. *Remote Sensing of Environment* **112**(4), 1614–1632 (2008).
68. Cheng, T., Rivard, B. & Sanchez-Azofeifa, A. Spectroscopic determination of leaf water content using continuous wavelet analysis. *Remote Sensing of Environment* **115**(2), 659–670 (2011).
69. Ryu, Y. *et al.* How to quantify tree leaf area index in an open savanna ecosystem: a multi-instrument and multi-model approach. *Agricultural and Forest Meteorology* **150**(1), 63–76 (2010).
70. Kühn, I., Durka, W. & Klotz, S. BiolFlor: a new plant-trait database as a tool for plant invasion ecology. *Diversity and Distributions* **10**(5), 363–365 (2004).
71. Hamilton, N. *ggtern: An Extension to 'ggplot2', for the Creation of Ternary Diagrams*. R package, 2(1) (2016).
72. Close, D. C. & Beadle, C. L. The ecophysiology of foliar anthocyanin. *The Botanical Review* **69**(2), 149–161 (2003).
73. Bondeau, A., Kicklighter, D. W. & Kaduk, J. Comparing global models of terrestrial net primary productivity (NPP): importance of vegetation structure on seasonal NPP estimates. *Global Change Biology* **5**, 35–45 (1999).
74. Niinemets, Ü. & Valladares, F. Photosynthetic acclimation to simultaneous and interacting environmental stresses along natural light gradients: optimality and constraints. *Plant Biology* **6**, 254–268 (2004).
75. Zeiger, E. The biology of stomatal guard cells. *Annual Review of Plant Physiology* **34**, 441–475 (1983).
76. Lawlor, D. W. & Cornic, G. Photosynthetic carbon assimilation and associated metabolism in relation to water deficits in higher plants. *Plant, Cell & Environment* **25**(2), 275–294 (2002).
77. Zarco-Tejada, P. J., Rueda, C. A. & Ustin, S. L. Water content estimation in vegetation with MODIS reflectance data and model inversion methods. *Remote Sensing of Environment* **85**(1), 109–124 (2003).
78. Niinemets, Ü. Global scale climatic controls of leaf dry mass per area, density, and thickness in trees and shrubs. *Ecology* **82**(2), 453–469 (2001).
79. Hättenschwiler, S. & Vitousek, P. M. The role of polyphenols in terrestrial ecosystem nutrient cycling. *Trends in Ecology & Evolution* **15**(6), 238–243 (2000).
80. Dormann, C. F. & Skarpe, C. Flowering, growth and defence in the two sexes: Consequences of herbivore exclusion for *Salix polaris*. *Functional Ecology* **16**(5), 649–656 (2002).

Acknowledgements

The project was funded by the German Aerospace Centre (DLR) on behalf of the Federal Ministry of Economics and Technology (BMW), FKZ 50 EE 1347. We would like to thank all employees of the botanical garden of the Karlsruhe Institute of Technology (KIT) for their generous support. The study has been supported by the TRY initiative on plant traits (<http://www.try-db.org>). The TRY initiative and database is hosted, developed and maintained by J. Kattge and G. Boenisch (Max Planck Institute for Biogeochemistry, Jena, Germany). TRY is currently supported by Future Earth/bioDISCOVERY and the German Centre for Integrative Biodiversity Research (iDiv) Halle-Jena-Leipzig. We acknowledge support by Deutsche Forschungsgemeinschaft and open access publishing fund of Karlsruhe Institute of Technology.

Author Contributions

T.K. performed the data acquisition. T.K. and S.S. performed the analysis and wrote the manuscript.

Additional Information

Supplementary information accompanies this paper at <https://doi.org/10.1038/s41598-019-43011-1>.

Competing Interests: The authors declare no competing interests.

Publisher's note: Springer Nature remains neutral with regard to jurisdictional claims in published maps and institutional affiliations.



Open Access This article is licensed under a Creative Commons Attribution 4.0 International License, which permits use, sharing, adaptation, distribution and reproduction in any medium or format, as long as you give appropriate credit to the original author(s) and the source, provide a link to the Creative Commons license, and indicate if changes were made. The images or other third party material in this article are included in the article's Creative Commons license, unless indicated otherwise in a credit line to the material. If material is not included in the article's Creative Commons license and your intended use is not permitted by statutory regulation or exceeds the permitted use, you will need to obtain permission directly from the copyright holder. To view a copy of this license, visit <http://creativecommons.org/licenses/by/4.0/>.

© The Author(s) 2019